ICNTC-2019 Special Issue

J. Indian Chem. Soc.,
Vol. 96, September 2019, pp. 1131-1136

Investigation of Mg, K, Cu, Zn doped S53P4 bioactive glass *in vitro* studies; bioactivity and biodegradability features

Cem Batuhan Cevlik, Ali Can Ozarslan, Burcu Karakuzu Ikizler, Yeliz Basaran Elalmis and Sevil Yücel*

Faculty of Chemical and Metallurgical Engineering, Department of Bioengineering, Yildiz Technical University, Esenler, Istanbul, Turkey

E-mail: syucel@yildiz.edu.tr, yuce.sevil@gmail.com

Manuscript received online 26 April 2019, revised and accepted 20 July 2019

In this study, it was aimed to produce by melt-quenching method non-additive (SiO_2-Na_2O-P_2O_5-CaO) and ion additive (SiO_2-Na_2O-P_2O_5-CaO-MgO-ZnO-K_2O-CuO) bioactive glasses (different forms; powder and granule). *In vitro* bioactivity and biodegradability properties of bioactive glasses in different forms (granule and powder) were examined with Simulated Body Fluid (SBF) and Tris-HCl analyses. Chemical bonds structures and surface morphology analysis of bioactive glasses (both additive and non-additive) were performed with FT-IR and SEM-EDS analysis before and after SBF immersion. SBF studies showed that both S53P4 bioactive glasses had similar bioactivity. As a results of Tris-HCl studies, *in vitro* biodegradability of bioactive glasses in powder forms are better than bioactive glasses in granule forms because of rapid raise of its pH value in Tris-HCl. However, ion additive S53P4 powder bioactive glass had more stable degradation behavior in comparison with non-additive S53P4 powder bioactive glass.

Keywords: Bioactive glass, doped, melt-quenching method, various forms, simulated body fluid.

Introduction

Bone grafts are frequently used in reconstruction of defects in bones to benefit from promoter and stimulating effects of bone formation. It is the ideal method to reconstruct the defect with another bone tissue of similar size, shape, and antigenic characteristics, although there are many alternative methods for reconstruction of bone defects[1–5].

In 1969, L. L. Hench discovered that the bone could form a chemical bond with some glass compositions. Biomaterials used as implants in the body until the discovery of bioactive glasses were bioinert materials such as metals and polymers, materials that could not form a stable interface with tissue, and formed undesirable effects such as fibrous encapsulation after implantation. Bioactive glasses are silica-based materials, and when they come into contact with body fluid, they exhibit a variety of chemical reactions that can bond to both soft and hard tissues quickly. The basic constituents of many bioactive glasses are SiO_2, Na_2O, CaO and P_2O_5 and fabricated by sol-gel method or melt-derived method[6]. First produced and most worked on is 45S5 with 45% SiO_2, 24.5% Na_2O, 24.4% CaO and 6% P_2O_5. Bioactive glasses produced after 45S5 bioactive glass are also named according to their composition. Other commercially available bone graft material compositions are S53P4 with 53% SiO_2, 23% Na_2O, 20% CaO, and 4% P_2O_5 [7]. The two US Food and Drug Administration (FDA) approved melt-derived compositions 45S5 and S53P4 consist of four oxides SiO_2, Na_2O, CaO and P_2O_5[8].

Different metal ions have crucial effects on bone formation as they act as enzymes or cofactors in bone metabolism or signaling pathways[9]. Magnesium is an essential element for metabolism that exist in human body. It is one of the most important mineral element in the bony matrix. Magnesium works as co-factor for many enzymes, and stabilizes the structures of DNA and RNA[10]. In the S53P4 bioactive glass composition by replaced the Na with K, several advantages achieved. Since K is heavier than Na, substitute of Na by bioactive glass system have a minimal change in density and microhardness values of the glass. In general, one of the glass networkers is potassium cations act as network modifiers and improved the breaking some Si-O-Si bonds due to assist disruption of the continuity of the glass net-

work, which leads to the form of non-bridging oxygen groups[11]. Zinc is a major trace element shown to have an important role in bone formation, both *in vitro* and *in vivo*. For growing of bone cell, zinc is fundamental for development and differentiation. Copper is a well-known antimicrobial material that can also contribute to bone generation through stimulation of osteogenesis and angiogenesis. Copper has been shown to be effective against both Gram-positive and Gram-negative bacteria and fungi[12].

In this study, we present the synthesis of potassium, zinc, magnesium and copper doped S53P4 and undoped S53P4 bioactive glasses by melt-quenching method. Both undoped and doped S53P4 bioactive glasses were characterized to determine chemical, structural and mechanical properties. Also bioactivity and biodegradability of bioactive glasses with different forms (granule and powder) were investigated with *in vitro* SBF and Tris-HCl studies. All results are compared to clarify the difference between undoped bioactive glass and doped bioactive glass.

Experimental

Materials:

Silicon dioxide (SiO_2) was obtained from Riedel-deHaën. Sodium bicarbonate ($NaHCO_3$), calcium carbonate ($CaCO_3$), sodium phosphate dibasic dihydrate ($Na_2HPO_4.2H_2O$), potassium phosphate dibasic trihydrate ($K_2HPO_4.3H_2O$), magnesium chloride hexahydrate ($MgCl_2.6H_2O$), zinc chloride ($ZnCl_2$) and copper(II) nitrate trihydrate ($Cu(NO_3)_2.3H_2O$) were supplied from Merck (Analytical grade, ≥ 99%).

Bioactive glass production:

Undoped S53P4 bioactive glass and doped S53P4 bioactive glass were produced by melt-quenching method and their compositions were given in Table 1. Briefly, prepared mixtures were melted in a high temperature furnace (Protherm, Turkey) using platinium crucible for 1 h at 1400°C and 2 h at 1450°C, respectively. The melted samples were casted onto counter for bead form and annealed at 450°C for 24 h. After annealing process, bead form bioactive glasses were broken in order to obtain smaller granules and stored in desiccator for analysis. Further, some granules were grinded in order to obtain bioactive glass powder and stored in desiccator for analysis.

Table 1. Composition of undoped bioactive glass and doped bioactive glass (wt%)

	SiO_2	Na_2O	CaO	P_2O_5	K_2O	CuO	MgO	ZnO
UDBG*	53	23	20	4	–	–	–	–
DBG*	53	19.8	20	4	2	0.3	0.8	0.02

*Abbreviations; UDBG: undoped bioactive glass, DBG: doped bioactive glass.

Characterization of produced bioactive glasses:

Vickers hardness and density measurements of bioactive glasses were performed using a microhardness tester (Bulut Makine Mikrobul 1000 D) and using density kit (Precisa 321 density kit), respectively. For Vickers harness analysis, all samples (0.3 *N*) were indented within 20 s. The values were converted to Vickers hardness numbers[13].

FT-IR spectra of UDBG and DBG samples were obtained by Shimadzu IR-Prestige 21 model FT-IR spectrophotometer with an ATR (attenuated total reflection) unit. Measurements were carried out at interval of 4000–650 cm^{-1}.

The morphology of doped and undoped bioactive glasses were examined using Scanning Electron Microscope (SEM, Zeiss Evo® Ls 10). Elucidation of the elemental structure on the doped and undoped bioactive glasses surface were analyzed with Energy Dispersive X-ray Spectrometry (EDS, Zeiss Evo® Ls 10).

In order to determine surface area and pore diameter of UDBG and DBG were analyzed with Nitrogen (N_2) Adsorption-Desorption (Micromeritics TRİSTAR II).

For biodegradability and bioactivity tests of both granule and powder forms, Tris-HCl solution and SBF solution studies were performed at 37±1°C for 7 days and for 14 days, respectively. Each doped and undoped bioactive glass samples were put in falcon tubes and incubated for 7 days at 37±1°C containing Tris-HCl solution (40 ml) for granule form (3 mm average diameter) and powder form (0.3 g) for biodegradability analysis. Likewise, each UDBG and DBG samples were also incubated in SBF solution at 37±1°C for 14 days (all SBF samples were refreshed for 14 days). The Tris-HCl and SBF solutions volumes were calculated based on equation in the literature[14]. Biodegradable behaviour of bioactive glasses were investigated depending on pH change of Tris-HCl solution. Alteration of surface morphology and hydroxyapatite or hydroxycarbonapatite (HA or HCA), an indicator of bioactivity, formation or accumulation on surface were detected by FT-IR and SEM-EDS analysis.

Results and discussion

Determination of bioactive glass density and Vickers hardness values:

Repeated measurements (n = 12) showed that the average density values of the undoped S53P4 bioactive glass and the doped S53P4 bioactive glass have the equal density value; 2.65 g/cm^3 in Table 2. These results demonstrated there was no difference in literature results of S53P4 bioactive glass density (2.66 g/cm^3) and different ion additive does not affect density of S53P4 bioactive glasses[15]. The Vickers hardness values of bioactive glasses produced by melt-quenching method were shown in Table 2. The Vickers hardness values of UDBG and DBG were measured to be 387 (HV) and 499 (HV) at the same indentation load, respectively. Results also revealed an evident variation in hardness values of DBG samples because of ion additive. Accordingly, doped S53P4 bioactive glass has better mechanical properties than undoped S53P4 bioactive glass.

Table 2. Density and Vickers hardness values of DBG and UDBG

	Density (g/cm^3)	Vickers hardness value (HV)
UDBG	2.65±0.02	387.8±19.9
DBG	2.65±0.02	499.5±4.4

Surface area, pore diameter, particle size analysis of bioactive glasses:

Specific BET surface area, pore volume and particle size results were given in Table 3. Any isothermal type is not corresponded for samples because the surface areas of both bioactive glass samples have a very low value. On the other hand, the specific BET surface areas of UDBG and DBG samples were measured as 0.071 (m^2/g), and 0.149 (m^2/g), respectively. The doped bioactive glass has more surface area than the undoped bioactive glass and the difference in surface area results of bioactive glasses may be related with ion addition. In addition, UDBG and DBG had almost same average pore diameter 0.35 nm. According to IUPAC, all bioactive glass have micropores (pore diameter: <2 nm) when considering the average pore diameter of both samples[16]. Based on this result, it can be estimated the ion addition does not change the pore diameters of bioactive glass. Furthermore, theoretical particle sizes (PS: μm) of the bioactive glasses may be calculated using the density (d: g/cm^3) and surface area (SA: m^2/g) analysis results in eq. (1)[17]. Doped bioactive glass (15 μm) has smaller particle size than undoped bioactive glass (31 μm).

Table 3. Specific BET surface area and pore diameter of DBG and UDBG

	Specific BET surface area (m^2/g)	Pore diameter (nm)	Particle size (μm)
UDBG	0.071	0.35	31
DBG	0.149	0.35	15

$$PS = \frac{6}{SA \times d} \quad (1)$$

Assessment of bioactivity of bioactive glasses:

The FT-IR spectra obtained from undoped bioactive glass and doped bioactive glass, before and after SBF soaking (during the first 7 days) are given in Fig. 1 and Fig. 2. Before SBF soaking, it has been found that the major bands seen at 1110–1120 cm^{-1} wavelength exhibit the Si-O stretching manner of vibration. The band around 910 cm^{-1} exhibits the Si-O-Si asymmetric strain in the samples[18]. The small broad band centered at between 3000–3600 cm^{-1} can be shown to hydroxyl group (-OH) in relation to moisture trapping and adsorbed water molecules. The band at nearly 694 cm^{-1} matches with Si-O-Si symmetric stretch of non-bridging oxygen atoms between silicate tetrahedra[19].

After soaking SBF both of UDBG and DBG samples with different peaks indicate a new structure formed on the sur-

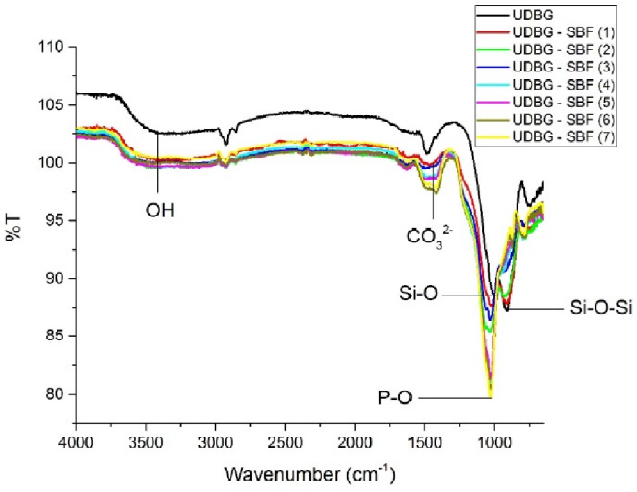

Fig. 1. FT-IR spectra of UDBG before and after SBF soaking.

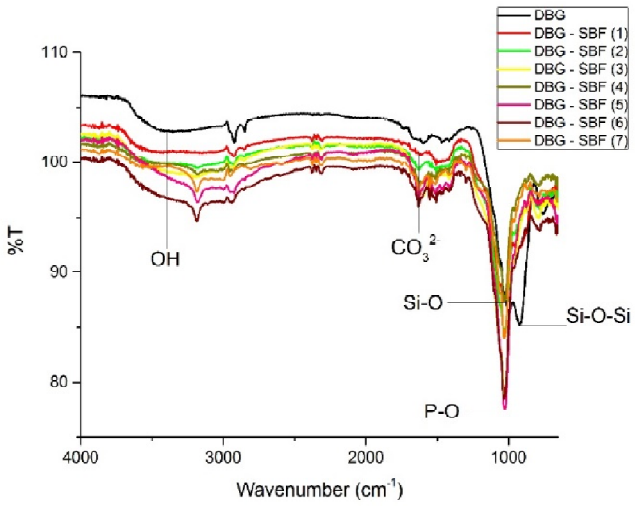

Fig. 2. FT-IR spectra of DBG before and after SBF soaking.

face of the samples. In the bioactive glasses, peaks at between 950–1050 cm^{-1} corresponding to P-O bonds are observed. This peak is not observed before the SBF soaking. Peaks between 950–1050 cm^{-1} corresponding to the P-O bond show the conversion of the calcium phosphate layer to the HCA on the surface of the samples. This result shows that HCA formation is increased as the waiting times of the samples in the simulated body fluid are increased. In the literature, the increase in peak intensities of the Na_2O-CaO-P_2O_5-SiO_2 system has been reported as the formation of P-O bonds around 1030 cm^{-1} and the increase in the waiting time in the simulated body fluid[20].

The SEM-EDS morphological and surface compositional analysis was performed on each UDBG and DBG granule samples before SBF soaking and after SBF incubation for

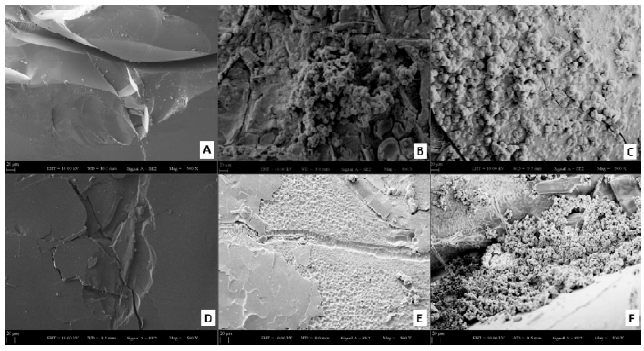

Fig. 3. SEM images (X500) of UDBG and DBG before and after SBF soaking (A: UDBG before SBF, B: UDBG after SBF 7. day, C: UDBG after SBF 14. day; D: DBG before SBF, E: DBG after 7. day, F: DBG after 14. day).

14 days (in Fig. 3). There is a uniform structure in the images before SBF immersion and all bioactive glasses surfaces have identical surface morphology. The surfaces of all samples are suitable for glass granule construction. HCA or HA layer formation clearly shown on UDBG and DBG granules surface after 7 days incubation in SBF according to SEM images. At the end of 14 days, the amount of HCA or HA gradually increased and then accumulation of HCA or HA occurred on the all bioactive glasses surface (surface morphological changes seen by SEM images). In addition to EDS results (in Table 4), the amount of calcium and phosphorus on the all bioactive glass surface increased significantly, and the amount of silica, sodium also decreased in time. These increasing and decreasing demonstrated the formation of HCA or HA on the bioactive glass surface (surface reactions)[21,22]. Likewise, as a result of EDS, it was calculated that the Ca/P ratios on the surface of UDBG samples are

Table 4. EDS results of undoped and doped S53P4 bioactive glasses before and after SBF soaking

	UDBG (Wt%)			DBG (Wt%)		
	Before SBF	SBF 7. day	SBF 14. day	Before SBF	SBF 7. day	SBF 14. Day
Si	24.76	2.26	1.98	24.76	2.51	0.88
Ca	14.28	47.16	52.06	14.28	27.49	36.56
Na	6.26	5.23	1.12	3.97	3.06	1.32
P	0.43	29.89	31.59	0.43	17.85	21.98
O	54.27	15.46	13.25	55.86	48.06	37.48
Mg	–	–	–	0.15	0.14	0.11
Cu	–	–	–	0.13	0.12	0.11
Zn	–	–	–	0.008	0.40	0.21
K	–	–	–	0.41	0.37	0.34

1.57 and 1.64 at the end of the 7. day and 14. day, respectively. DBG samples were calculated to be 1.54 at the 7. day and 1.66 at the end of the 14. day. These values are similar the Ca/P = 1.5–1.667 value range required for the formation of the hydroxyapatite phase, indicating that the surface coated HCA or HA layer[23]. The Ca/P ratio detected at the surface of the bioactive glass sample proves the presence of the HCA or HA layer detected in the SEM images. Thus, undoped and doped S53P4 bioactive glass exhibit good bioactivity properties. However, there is no difference between UDBG and DBG bioactivity because of ion additive.

Biodegradable behaviour of bioactive glasses:

As shown as Fig. 4, both of UDBG and DBG granule and powder samples showed significant value differences when the pH values were compared over time (up to 7 days). pH values increasing is the evidence for the biodegradability of the all bioactive glass samples. Based on these significant pH differences between granule and powder forms of all

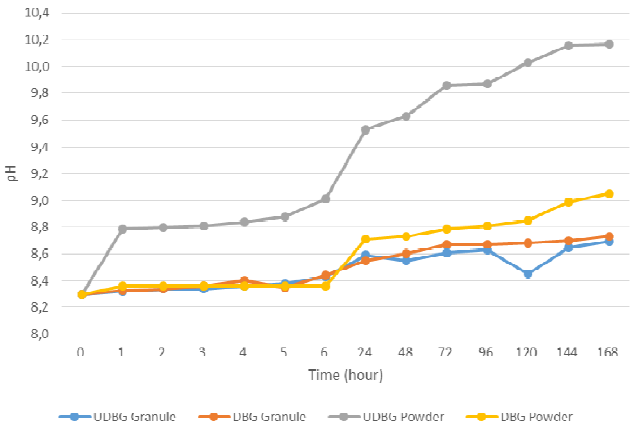

Fig. 4. pH values change of UDBG and DBG in Tris-HCl incubation for 7 days.

bioactive glasses, that is conceivable, the surface area is major effect at dissolving of the material. Compare the pH changes of the all forms, granule samples have minor increasing, in opposite to powder samples have major increasing after 6 h. At the end of first hour, especially powder UDBG has sharply pH raise because of its high degradability. The results are also proofing, the powder forms have abundant biodegradability than granule forms for both UDBG and DBG samples. Considering the all granule samples pH changing in the time, both of UDBG and DBG granules have nearly same pH value during the all incubation time. Comparing the both of powder samples pH changing in the time, the significant change in pH value is observed the UDBG powder sample, in addition the DBG powder sample has not enough differences as the UDBG powder sample in pH values. Based on the results of the powder samples, it may be considered that the ion additive have an adverse effect on the dissolution in the powder sample.

Conclusions

Granule and powder form S53P4 bioactive glasses containing potassium, zinc, magnesium and copper were prepared by melt-quenching method. Structural changes were compared with non-additive S53P4 bioactive glass and ion additive S53P4 bioactive glass *in vitro* studies. Similar bioactivity and biodegradability properties were observed for both granule S53P4 bioactive glasses with the same density (2.65 g/cm^3). However, powder S53P4 bioactive glasses (both non-additive and ion additive) had higher degradability in Tris-HCl. Furthermore, ion additive S53P4 bioactive glass with powder form had more stable degradation behavior in comparison with non-additive S53P4 bioactive glass. HA or HCA formation and accumulation within 7 day and 14 day in SBF were observed according to SEM-EDS analysis. Based on the structural analysis and *in vitro* studies results, it is possible to conclude that the ion additive S53P4 bioactive glasses with granule form and powder form investigated in this study could find applications as hard tissue regeneration material in bone tissue engineering.

References

1. W. J. O'brien, Quintessence Publishing Co., Inc., 1997.
2. R. Z. Legeros and R. G. Craig, *Journal of Bone and Mineral Research*, 1993. 8.
3. R. Sanders, *The Journal of Bone and Joint Surgery*, 2007, **89**, 3.469.
4. O. Faour, R. Dimitriou, C. A. Cousins and P. V. Giannoudis, *Injury*, 2011, **42**, S87.
5. P. V. Giannoudis, H. Dinopoulos and E. Tsiridis, *Injury*, 2005, **36(3)**, S20.
6. J. R. Jones, L. M. Ehrenfried and L. L. Hench, *Biomaterials*, 2006, **27**, 964.
7. L. L. Hench, *New Journal of Glass and Ceramics*, 2013, **3(02)**, 67.
8. L. Hupa, Woodhead Publishing Series in Biomaterials, 2011, pp. 3-28.

9. A. Hoppe, N. S. Güldal and A. R. Boccaccini, *Biomaterials*, 2011, **32(11)**, 2757.
10. E. Dietrich, H. Oudadesse, A. Lucas Girot and M. Mami, *Journal of Biomedical Materials Research, Part A*, 2009, **88(4)**, 1087.
11. A. Marikani, A. Maheswaran, M. Premanathan and L. Amalraj, *Journal of Non-Crystalline Solids*, 2008, **354(33)**, 3929.
12. C. Wu, Y. Zhou, M. Xu, P. Han, L. Chen, J. Chang and Y. Xiao, *Biomaterials*, 2013, **34**, 422.
13. S. Türker and T. Biskin, *Journal of Oral Rehabilitation*, 2002, **29(7)**, 657.
14. T. Kokubo and H. Takadama, *Biomaterials*, 2006, **27(15)**, 2907.
15. J. Massera and L. Hupa, *Journal of Materials Science: Materials in Medicine*, 2014, **25(3)**, 657.
16. D. H. Everett, Appendix 2, Part 1, *Colloid Surf. Sci., Pure Appl. Chem.*, 1972, **31**, 578.
17. C. Piccirillo, R. C. Pullar, E. Costa, A. Santos-Silva, M. M. E. Pintado and P. M. L. Castro, *Materials Science and Engineering C*, 2015, **51**, 309.
18. A. C. Ozarslan and S. Yucel, *Materials Science and Engineering C*, 2016, S0928-4931(16)30571-9.
19. V. K. Vyas, A. S. Kumar, A. Ali, S. Prasad, P. Srivastava, S. P. Mallick, M. Ershad, S. P. Singh and R. Pyare, *Boletín De La Sociedad Española De Cerámica Y Vidrio*, 2016, **55(6)**, 228.
20. S. Hesaraki, M. Alizadeh, H. Nazarian and D. Sharifi, *Journal of Material Science: Materials in Medicine*, 2010, **21**, 695.
21. L. L. Hench and H. A. Paschall, *Journal of Biomedical Materials Research*, 1974, **8**, 49.
22. L. L. Hench, *Journal of Material Science: Materials in Medicine*, 2006, **17**, 967.
23. N. Eliaz and N. Metoki, *Materials (Basel)*, 2017, **10(4)**, 334.